

Numerical Test of Disk Trial Wave function for Half-Filled Landau Level

S.-R. Eric Yang

*Department of Physics, Korea University, Seoul 136-701, Korea
Asia Pacific Center for Theoretical Physics, Seoul, Korea*

Min-Chul Cha

Department of Physics, Hanyang University, Ansan 425-791, Korea

Jung Hoon Han

Department of Physics, U.C. Berkeley, Berkeley, CA 94720 USA

The analyticity of the lowest Landau level wave functions and the relation between filling factor and the total angular momentum severely limits the possible forms of trial wave functions of a disk of electrons subject to a strong perpendicular magnetic field. For N , the number of electrons, up to 12 we have tested these disk trial wave functions for the half filled Landau level using Monte Carlo and exact diagonalization methods. The agreement between the results for the occupation numbers and ground state energies obtained from these two methods is excellent. We have also compared the profile of the occupation number near the edge with that obtained from a field-theoretical method. The results give qualitatively identical edge profiles. Experimental consequences are briefly discussed.

I. INTRODUCTION

There has been a great interest in two-dimensional electron liquid in a strong magnetic field at half-filling. Its bulk properties have been investigated and several novel features have been revealed^{1-4,6,5}. Electrons form a new exotic metal in which they move effectively in zero magnetic field despite the presence of an external field¹. A dipole-like new particle^{2-4,6,5} with fermionic statistics has been introduced. This new state of matter forms a Fermi liquid with a finite compressibility⁷.

The edge properties of this exotic liquid are of great current interest, both experimentally⁸ and theoretically⁹⁻¹⁴. Recently a two-mode model for the edge¹⁰ has been proposed based on a theory of the electron liquid at $\nu = 1/2$ consisting of charged Bose and neutral Fermi liquids⁶. In this theory the charge mode propagates while the neutral mode is dispersion-less. A theory based on the topology of Abelian fractional quantum Hall states also leads to similar results, but in this approach two non-propagating modes of a purely topological origin exist¹¹.

A disk of electrons consists of a bulk and an edge, and it is desirable to treat them in the same theoretical framework. The edge and bulk properties have been also investigated using a trial wave function for an electron disk at half-filling¹²⁻¹⁴. The trial wave function was constructed using analyticity of the lowest Landau level wave functions, and the fact that the filling factor (ν) is related to the total angular momentum (M_z) through $\nu = N(N-1)/2M_z$. These conditions severely limit the possible forms of the wave function^{12,13}. It was tested that the wave function overlap of this state with the exact one is essentially one for $N = 5$ ¹⁴. The computed edge occupation number showed, in sharp contrast to incompressible Laughlin states, that a tail exists in the occupation number beyond the radius of a droplet of uniform filling factor $1/2$ ¹³. The properties of zeroes of the wave functions have been also investigated¹³. The proposed trial wave function can be used to understand the dynamic structure factor, which is a physically measurable quantity. This was done by constructing trial wave functions for some of the low energy excitations of a disk¹⁴. One of them is the center of mass (CM) motion, which can be interpreted as an edge mode. Other excitations are identified and their wave functions are also constructed. They are not edge modes, but are excitations of the entire droplet. They are new excitations of a droplet at $\nu = 1/2$ which do not exist in incompressible states. The dynamic structure factor shows that the disk can support several low energy excitations, unlike incompressible quantum Hall states.

In this paper we perform an extensive numerical test of the proposed trial wave functions for an electron disk at half-filling. We find that the previously proposed trial wave functions^{12,13} work quite well up to $N = 8$. We find that for bigger values of N almost degenerate states with lower energies exist. Using these trial wave functions we have computed several physical properties by performing Monte Carlo simulations, and have tested the obtained results against exact diagonalization results for up to $N = 12$. The agreement between the results for the occupation numbers and ground state energies obtained from these two methods is excellent. We have also compared the profile of the occupation number near the edge with that of a field theoretical approach^{10,11}. They give qualitatively identical edge profiles.

This paper is organized as follows. In Sec. II we explain the composite Fermion wave function, which is a central concept in our trial wave function approach. Next, in Sec. III, we give the physical idea behind the construction of trial wave functions at the principal filling factors using composite Fermion wave functions. In Sec. IV we perform Monte Carlo simulations using the proposed trial wave functions and compared the extracted physical properties with those of exact diagonalization method. A field theoretical calculation of the edge occupation number is carried out in Sec. V and the obtained result is compared with those of the exact diagonalization and Monte Carlo results. Discussions are given in Sec. VI. In this paper length and energy are measured in units of ℓ and $e^2/\epsilon\ell$, where ℓ is the magnetic length.

II. COMPOSITE FERMION WAVE FUNCTIONS

In this section we explain composite fermion wave function, which is a central concept in our trial wave function approach. This concept was introduced by Jain and Kamila¹⁵. Before we discuss our trial wave function approach it is necessary to understand this concept first. So we give a short summary of their result.

A. Physical Model of a Disk

Let us first set up our model of a disk. We consider a system of 2D electrons confined by a parabolic potential, $V(r) = m_e \Omega^2 r^2 / 2$. The advantage of this model is that some exactly known results can be utilized in constructing the collective modes. Such a system will form a uniform density electron disk for sufficiently large N . The symmetric gauge single-particle eigenstates $\phi_{n,m}(z)$ are conveniently classified by a Landau level index n and an angular momentum index $m = -n, -n+1, \dots$ ($z = x + iy$). In the strong field limit the single particle orbitals in the $n = 0$ level have energies $\epsilon_m = \hbar\omega_c/2 + \gamma(m+1)$, where $\gamma = m_e \Omega^2 \ell^2$. The system is invariant under spatial rotations about an axis perpendicular to the 2D plane and passing through the center of the dot. It follows that the total angular momentum M_z is a good quantum number. Eigenenergies may be expressed as a sum of interaction and single-particle contributions

$$E_i(N, M_z) = U_i(N, M_z) + \gamma(N + M_z). \quad (1)$$

Here i labels a state within a M_z subspace, and $U_i(N, M_z) \propto e^2/\epsilon\ell$ is determined by exactly diagonalizing the electron-electron interaction term in the Hamiltonian within this subspace. We will present in this paper a different approach than some of previous works on fractional quantum Hall states disk geometry^{16,17}.

B. Composite Fermion Wave functions

Recently it has been argued that the main physics of strong electron correlation in quantum Hall systems is that the electrons carry two Jastrow factors¹⁸.

$$\psi[z] = P_{L^3} \prod_{j < k} (z_j - z_k)^2 \begin{vmatrix} \phi_{n_1 m_1}(z_1) & \dots & \phi_{n_1 m_1}(z_N) \\ \dots & \dots & \dots \\ \phi_{n_N m_N}(z_1) & \dots & \phi_{n_N m_N}(z_N) \end{vmatrix} \quad (2)$$

where P_{L^3} stands for projection to the lowest Landau level (LLL). It is useful to rewrite this as

$$\psi[z] = P_{L^3} \begin{vmatrix} \phi_{n_1 m_1}(z_1) J_1 & \dots & \phi_{n_1 m_1}(z_N) J_N \\ \dots & \dots & \dots \\ \phi_{n_N m_N}(z_1) J_1 & \dots & \phi_{n_N m_N}(z_N) J_N \end{vmatrix} \quad (3)$$

In physical terms, the Jastrow factor $J_i = \prod_{k \neq i} (z_i - z_k)$ implies that each particle carries with it a correlation hole with respect to all the other particles.

The projection P_{L^3} is tantamount to replacing the anti-holomorphic variable \bar{z} with $2(\partial/\partial z)$ ¹⁹. It is not straightforward to project this wave function to the LLL. Jain and Kamila (JK)¹⁵ have proposed the following wave functions of interacting fermions in the LLL for a given total angular momentum M_z :

$$\Psi^{CF} = \begin{vmatrix} \eta_{n_1 m_1}(z_1) & \dots & \eta_{n_1 m_1}(z_N) \\ \dots & \dots & \dots \\ \eta_{n_N m_N}(z_1) & \dots & \eta_{n_N m_N}(z_N) \end{vmatrix} \quad (4)$$

$$\eta_{nm}(z_i) = e^{-\frac{1}{4}|z_i|^2} z_i^{m+n} \partial_i^n J_i \quad (5)$$

$\eta_{nm}(z)$ is *not* a genuine single-particle state as its value depends on the position of all the other particles. Nonetheless to stress the similarity between Eq.(3) and Eq.(4) JK regard n and m as the LL index and the angular momentum of the composite fermions (CFs), respectively. The composite fermion Landau level (CFLL) index is just a convenient nomenclature for some abstract mathematical property of $\eta_{nm}(z)$. *It should be noted that CFLL index n is not a real Landau level index, and although higher CFLL indices appear in this wave function it lies entirely in the lowest electron Landau level.* On the other hand, it can be shown that the total angular momentum of Ψ_{CF} is $M_z = N(N-1) + M^*$, where $M^* = \sum_i m_i$ is the sum over angular momentum of CF levels ($N(N-1)$ stems from N Jastrow factors of J_i).

JK choose the ground state as the compact state $[N_0, N_1, \dots, N_{l-1}]$, where the number of CFs in the i -th CFLL is N_i . This state is defined to satisfy: [1] $N_0 \geq N_1 \geq N_2, \dots$; [2] $\sum_{i=0}^{l-1} N_i = N$; [3] For given N_i , all the CF levels $m = -i, -i+1, \dots, N_i - i - 1$ are assumed to be occupied. For example, for $N_i = 5$ the CF occupation numbers are given by $(\bullet, \bullet, \bullet, \bullet, \bullet, \circ, \circ, \dots)$ in the i -th CFLL [An occupied (unoccupied) CF state is represented by a full (empty) circle. The angular momentum of a CF state increases from left to right]. The ultimate justification of choosing these wave functions comes from the comparison with exact diagonalization results (See Sec. IV.B.1 Wave function overlaps).

We will drop the universal factor $\prod_i e^{-|z_i|^2/4}$ from now on. When we write out the wave function of $[N_0, N_1, \dots, N_{l-1}]$ it has the form

$$\begin{vmatrix} J_1 & z_1 J_1 & \dots & z_1^{N_0-1} J_1 & \partial_1 J_1 & \dots & z_1^{N_1-1} \partial_1 J_1 & \dots \\ J_2 & z_2 J_2 & \dots & z_2^{N_0-1} J_2 & \partial_2 J_2 & \dots & z_2^{N_1-1} \partial_2 J_2 & \dots \\ \dots & \dots & \dots & \dots & \dots & \dots & \dots & \dots \\ J_N & z_N J_N & \dots & z_N^{N_0-1} J_N & \partial_N J_N & \dots & z_N^{N_1-1} \partial_N J_N & \dots \end{vmatrix}. \quad (6)$$

Successively higher powers of ∂_i acting on J_i appear as we move to the right for a given row. The matrix elements are of the form $z_i^{n+m} \partial_i^n J_i$. One can easily verify that the $1/3$ Laughlin state²⁰ is given, in this notation, by $[N_0, N_1, \dots, N_{l-1}] = [N, 0, \dots, 0]$:

$$\begin{vmatrix} J_1 & z_1 J_1 & \dots & z_1^{N-1} J_1 \\ \dots & \dots & \dots & \dots \\ J_N & z_N J_N & \dots & z_N^{N-1} J_N \end{vmatrix} \quad (7)$$

It can also be verified that the wave function for the filled electronic Landau level at $\nu = 1$ is given by $[N_0, N_1, \dots, N_{l-1}] = [1, 1, \dots, 1]$:

$$\begin{vmatrix} J_1 & \partial_1 J_1 & \dots & \partial_1^{N-1} J_1 \\ \dots & \dots & \dots & \dots \\ J_N & \partial_N J_N & \dots & \partial_N^{N-1} J_N \end{vmatrix} \quad (8)$$

JK do not give specific prescription for other general filling factors.

III. CONSTRUCTION OF TRIAL WAVE FUNCTIONS FOR PRINCIPLE FILLING FACTORS

Now that we have explained the composite fermion wave functions we can proceed to construct trial wave functions at other principal filling factors.

A. Uniform density droplet

The formula $\nu = N(N-1)/2M_z$, which relates the filling factor to the total angular momentum can be shown to be true for Laughlin states using plasma analogy²⁰. For other states described by composite fermion wave functions numerical results support the validity of this formula. We have tested numerically the wave functions $[4, 3, 3, 1]$ and $[6, 4, 3, 2, 1, 1]$, which we believe describe the $\nu = 1/2$ state at $N = 11$ and $N = 17$, respectively. We have verified for these states that the average electron density $n(r)$ inside dot is approximately $(1/2\pi\ell^2)\nu$ (see Fig. 1). We have also tested other states $[6, 1, \dots, 1]$ and $[9, 1, \dots, 1]$ for $N = 11$ and $N = 17$ and found similar results. We expect from the size dependence that the agreement should become better for $N \gg 17$ (17 is the biggest size we could handle numerically). Even for the Laughlin states numerical results show that the correct average value is approached slowly as N increases²¹.

B. First method

Let us first explain our trial wave function approach using analyticity of the lowest Landau level wave functions and the fact that the filling factor is related to the total angular momentum.

As a trial wave function for the state at $\nu = 1/2$ Yang and Han^{12,13} have proposed the state $[N/2, 2, 1, \dots, 1]$ ($[(N-1)/2, 1, \dots, 1]$) for even (odd) N . It can be verified that for each value of $N = 3, 4, 5, 6, 7$ this state is the *only* possible compact state satisfying the condition $\nu = N(N-1)/2M_z$. The occupation of CFs in these states are listed in Table I. The state $[\frac{N}{2}, 2, 1, \dots, 1]$ has the form

$$\Phi'_0 = \begin{vmatrix} J_1 & z_1 J_1 & \dots & z_1^{\frac{N}{2}-1} J_1 & \partial_1 J_1 & \dots & \partial_1^{\frac{N}{2}-1} J_1 \\ \dots & \dots & \dots & \dots & \dots & \dots & \dots \\ J_N & z_N J_N & \dots & z_N^{\frac{N}{2}-1} J_N & \partial_N J_N & \dots & \partial_N^{\frac{N}{2}-1} J_N \end{vmatrix} \quad (9)$$

This state has the following form in terms of antiholomorphic variable \bar{z}

$$\begin{vmatrix} J_1 & z_1 J_1 & \dots & z_1^{\frac{N}{2}-1} J_1 & \bar{z}_1 J_1 & \dots & \bar{z}_1^{\frac{N}{2}-1} J_1 \\ \dots & \dots & \dots & \dots & \dots & \dots & \dots \\ J_N & z_N J_N & \dots & z_N^{\frac{N}{2}-1} J_N & \bar{z}_N J_N & \dots & \bar{z}_N^{\frac{N}{2}-1} J_N \end{vmatrix} \quad (10)$$

Han and Yang¹³ have also proposed trial wave functions at other principal filling factors.

C. Second method

The proposed wave functions can be also constructed using a more physical argument based on counting flux numbers and their relation to the total angular momentum.

Consider the $\nu = 1/3$ state $[N]$, which has $3N$ flux quanta. The angular momentum of this state is $3N(N-1)/2$. If two flux quanta are removed from this state the number of flux quanta per particle will be $1/\nu' = \frac{3N-2}{N}$. Then, in the large N limit, the total angular momentum will be given by

$$M_z = \frac{1}{\nu'} N(N-1)/2 = 3N(N-1)/2 - (N-1) \approx 3N(N-1)/2 - N. \quad (11)$$

From this we see that reducing two flux quanta amounts to reducing the total angular momentum by N . The resulting state is $[N-1, 1]$ since the angular momentum of this state is $N(N-1) + M^* = 3N(N-1)/2 - N$. Here we have used the fact that the total angular momentum of composite fermions M^* in the state $[N-1, 1]$ is $-1 + \sum_{i=0}^{N-2} m_i = -1 + (N-1)(N-2)/2$. If two flux quanta are removed additionally, the angular momentum is again reduced by N and the resulting state is $[N-2, 1, 1]$. If two flux are removed q times successively the resulting state will be $[N-q, 1, 1, \dots, 1]$, where 1 appears q times (However, this state is not unique. For other possibilities, see below). The total angular momentum of this state is $3N(N-1)/2 - Nq$. The half filled state has $M_z = N(N-1)$ so $q = (N-1)/2$. For the $\nu = 2/3$ state $M_z = 3N(N-1)/4$ so $q = 3(N-1)/2$. For $\nu = n/(2n \pm 1)$ we find $q = \frac{(N-1)}{2}(3 - \frac{1}{\nu})$.

D. Trial wave functions for $N \geq 9$

As the number of electrons increases, other choices of occupations are allowed than proposed previously. For $\nu = 1/2$, unlike the case for $N \leq 7$, there are two possible compact states at $N = 8$ with the correct value of $M_z = N(N-1) + M^*$: The first state is $[4, 2, 1, 1]$ with occupied CF states $(n, m) = (0, 0), (0, 1), (0, 2), (0, 3), (1, -1), (1, 0), (2, -2), (3, -3)$, and the second state is $[3, 3, 2]$ with $(n, m) = (0, 0), (0, 1), (0, 2), (1, -1), (1, 0), (1, 1), (2, -2), (2, -1)$ (in both cases $\sum_i m_i = M^* = 0$). Note that the second state does not have the proposed form $[N/2, 2, 1, \dots, 1]$, but it also turns out its energy is almost degenerate with that of $[4, 2, 1, 1]$ (the energies are 6.025 vs. 6.095). For $\nu = 1/2$, the possible choices of $[N_0, N_1, \dots]$ are given in the Table I for several values of N . Possible choices $[N_0, N_1, \dots]$ at other principal values of ν are given in Table II. The Monte Carlo energies of these states at $\nu = 1/2$ are given in Table I. We choose the state with the lowest energy as the groundstate.

IV. MONTE CARLO AND EXACT DIAGONALIZATION RESULTS

Ground state properties can be calculated from the proposed trial wave functions. Here we concentrate on occupation numbers and ground state energies.

A. Monte Carlo calculation of occupation numbers

For Laughlin states the edge occupation number $n(k) \sim (k - k_{ed})^{(1/\nu-1)21-24}$. In disk geometry single particle angular momentum m is related to the wave vector through $k = 2\pi m/R_m$, where $R_m = \sqrt{2(m+1)}$. The value of m corresponding to the location of the edge is $m_{ed} = 2N - 1^{12}$ for $\nu = 1/2$. The corresponding k is defined as k_{ed} . The exponent, $1/\nu$, in this expression is intimately related to the short range correlations of the Laughlin liquid. Therefore one can expect to gain information about the the short range correlations from the edge occupation numbers. This is the motivation for investigating occupation numbers.

Now we evaluate the one-particle density matrix $n(z, z')$, which is defined as

$$n(z, z') = N \int d^2 z_2 \cdots d^2 z_N \psi^*(z, z_2, \cdots, z_N) \psi(z', z_2, \cdots, z_N) / Q_N, \quad (12)$$

where the normalization integral is $Q_N = \langle \psi | \psi \rangle$. We are especially interested in the angular dependence of the one-particle density matrix, $n(r, re^{i\theta})$, where $r = |z|$. Using $n(r, re^{i\theta}) = \int d^2 z_1 (1/2\pi |z_1|) \delta(|z_1| - r) n(z_1, z_1 e^{i\theta})$, we have

$$n(r, re^{i\theta}) = \sum_i \int d^2 z_1 \cdots d^2 z_N \frac{\delta(|z_i| - r)}{2\pi |z_i|} \psi^*(z_1, \cdots, z_i, \cdots, z_N) \psi(z_1, \cdots, z_i e^{i\theta}, \cdots, z_N) / Q_N, \quad (13)$$

It is convenient to perform the integration by Monte Carlo sampling with the probability distribution $P(z_1, z_2, \cdots, z_N) = |\psi(z_1, z_2, \cdots, z_N)|^2 / \langle \psi | \psi \rangle$, so that

$$n(r, re^{i\theta}) = \sum_i \int d^2 z_1 \cdots d^2 z_N \frac{\delta(|z_i| - r)}{2\pi |z_i|} \frac{\psi(z_1, z_2, \cdots, z_i e^{i\theta}, \cdots, z_N)}{\psi(z_1, z_2, \cdots, z_i, \cdots, z_N)} P(z_1, z_2, \cdots, z_N). \quad (14)$$

The angular-momentum occupation number is determined²¹ by

$$n_m = \frac{1}{|\phi_m(r)|^2} \sum_{j=0}^{m_{eff}} \frac{e^{i\theta_j} m n(r, re^{i\theta_j})}{m_{eff} + 1}, \quad (15)$$

where m_{eff} is the highest power of z_i , and

$$|\phi_m(r)|^2 = \frac{1}{2\pi m!} \frac{r^{2m}}{2^m} e^{-r^2/2}. \quad (16)$$

The interaction energy can also be estimated from these wave functions. The interacting part of the the Hamiltonian is

$$H = \sum_{i>j} \frac{1}{|z_i - z_j|}. \quad (17)$$

Monte Carlo sampling has been carried out through Metropolis algorithm by changing the position of electrons, $z_i \rightarrow z_i + \delta z_i$, where typically $|\delta z_i| \leq 0.2 - 0.4$. The wave functions vary rapidly with respect to the positions of electrons so that after one Monte Carlo sweep $|\psi|_{\text{new}}^2 / |\psi|_{\text{old}}^2$ changes up to $\sim 10^{10}$ or 10^{-10} . It is remarkable that, in spite of this rapid variation of the wave functions, Monte Carlo method quite nicely gives accurate expectation values.

B. Numerical Results

1. Wave function overlaps

The justification of the proposed wave functions at $\nu = 1/2$ comes from small-size exact diagonalization. For $N = 5$ and for the Coulomb interaction the overlap of this ground state wave function with the exact wave function is 0.9989¹⁴. (The accuracy of the proposed trial wave function is comparable to that of the Laughlin state: for four particles with Coulombic repulsions the overlap is 0.979 for the $\nu = 1/3$ Laughlin state²⁰). For $N = 5$ trial wave functions of the first, second, and third excited states with the change in the total angular momentum $\delta M_z = 1$ can be constructed from the ground state wavefunction. The overlaps with the exact ones are 0.9990, 0.9663, and 0.9098, respectively¹⁴.

2. Occupation numbers and ground state energies

For N bigger than 5 the proposed wave function of Eq.(9) can be tested against the exact diagonalization results by comparing the occupation numbers.

Fig. 2 displays occupation numbers for $\nu = 1/3$ disk. The results obtained from the Laughlin wave function and those obtained from exact diagonalizations are shown. The agreement between the two are excellent near the edge. This implies that the Laughlin wave function captures the short range correlations remarkably well. Note that near the center of the disk a small discrepancy exists between the results of Laughlin wave function and exact diagonalization.

Fig. 3 displays occupation numbers for $\nu = 1/2$ disk, calculated using Eq.(9). Again, as in the case of the Laughlin wave function, the results obtained from the proposed trial wave function and those of the exact diagonalization are in excellent agreement. For $N = 8$ the state $[3, 3, 2]$ has the correct angular momentum consistent with $\nu = 1/2$, but its occupation numbers show a significant deviation from the exact ones even near the edge. In contrast the state $[4, 2, 1, 1]$, given by Eq.(9), agrees with the exact results. For $N = 9$ the energies for two possible wavefunctions $[5, 1, 1, 1, 1]$ and $[3, 3, 3]$ are nearly the same, deviating from the exact diagonalization result by about 1%. We find neither $[5, 1, 1, 1, 1]$ nor $[3, 3, 3]$ give accurate occupation numbers. In this case even the exact diagonalization procedure converges very slowly. Probably an elaborated linear combination of wave functions could lower the energy. For $N = 10, 11, 12$, we find, among possible choices of wave functions, that the results of the lowest energy states agree with the exact diagonalization result (see Table I and Fig. 4). Note that exact diagonalization results are not available for $N \geq 13$.

3. Zeroes of wavefunction

For $N = 12$ the trial wavefunction $[5, 3, 2, 1, 1]$ has the lowest Monte Carlo energy. We have investigated zeroes of this trial wavefunction (see Fig.5). We find that in $[5, 3, 2, 1, 1]$ zeroes are closer to the electrons in comparison to $[6, 2, 1, 1, 1, 1]$. This is consistent with the fact that $[5, 3, 2, 1, 1]$ has lower energy than $[6, 2, 1, 1, 1, 1]$. Properties of zeroes of other trial wavefunctions are discussed at length in Han and Yang¹³.

V. FIELD THEORETICAL CALCULATION OF OCCUPATION NUMBERS

Small-size exact diagonalization calculation at $\nu = 1/2$ indicates that $n(k)$ near the edge depends linearly on k for $k \leq k_{ed}$ ¹². We investigate using a field theoretical approach whether this feature survives in the thermodynamic limit. The hydrodynamic action for the edge mode of a half-filled droplet has been written down by Lee and Wen¹⁰, and independently by Lopez and Fradkin¹¹. Ignoring the coupling to the bulk degrees of freedom, the action is given by

$$S_{edge} = \frac{1}{2\pi} \int \frac{d\phi}{dx} \left(\frac{d\phi}{dt} - v_c \frac{d\phi}{dx} \right) dx dt - \frac{1}{4\pi} \int \frac{d\eta}{dx} \left(\frac{d\eta}{dt} + v_n \frac{d\eta}{dx} \right) dx dt, \quad (18)$$

where $\partial_x \phi$ and $\partial_x \eta$ are the displacement fields of the charge mode and the neutral mode. Following Lopez and Fradkin's approach one would have to add another neutral mode in the action. The results for the occupation number remain unaltered, and we choose to present our result with the two-mode model for simplicity. The boson fields $\phi(x)$ and $\eta(x)$ satisfy the following commutation relation

$$\left[\frac{d\phi}{dx}, \phi(y) \right] = \pi i \delta(x - y); \quad \left[\frac{d\eta}{dx}, \eta(y) \right] = -2\pi i \delta(x - y). \quad (19)$$

The electron operators are constructed as^{10,11}

$$\psi_e(x) \sim e^{-2i\phi(x) \pm i\eta(x)}. \quad (20)$$

One can verify that the operators satisfy the necessary anticommutation relations.

The occupation number profile follows from the equal-time single-particle Green's function, $G_e(x) = \langle \psi_e^\dagger(x) \psi_e(0) \rangle$. Since the dynamics of ϕ and η are independent, one obtains

$$G_e(x) \sim \exp[G_\phi(x) + G_\eta(x)] \quad (21)$$

where

$$\begin{aligned} G_\phi(x) &= -2 \ln \left(\frac{1 - \exp[-2\pi(1 - ix\Lambda_c)/\Lambda_c L]}{1 - \exp[-2\pi/\Lambda_c L]} \right), \\ G_\eta(x) &= -\ln \left(\frac{1 - \exp[-2\pi(1 + ix\Lambda_n)/\Lambda_n L]}{1 - \exp[-2\pi/\Lambda_n L]} \right) \end{aligned} \quad (22)$$

are equal-time Green's functions of ϕ and η . A finite circumference L of the droplet has been introduced, as well as some high momentum cut-off Λ_c/Λ_n for charged/neutral modes.

A Fourier transform of Eq. (21) should give the momentum occupation number. But it is first necessary to define the position of the edge. It is natural to define the position of the edge as m_{ed} from the following simple model for the edge: Consider a disk of electrons at half filling with uniform occupation numbers given by $n(m) = 1/2(0)$ for $m \leq m_{ed}$ (*else*). The sum over occupied $n(m)$ is N so $m_{ed} = 2N - 1$. A uniform disk at $\nu = 1/3$ has the occupation numbers given by $n(m) = 1/3(0)$ for $m \leq 3N - 1$ ($m > 3N - 1$), implying that the edge is at $m_{ed} = 3N - 1$. We have used these values of m_{ed} as the positions of the edges. In real systems effects neglected in this simple model will change the shape of occupation number around the edge. At half filling accurate numerical results demonstrate that the occupation number is smeared out around $m_{ed} = 2N - 1$, just like at the edge of an ordinary metal. As Yang and Han¹² pointed out this definition of the location of the edge gives a good scaling curve (data collapse) for the edge profile for different values of N (other definitions will fail). In the $\nu = 1/3$ incompressible (non-metallic) case, the shape of occupation number around the edge is changed differently: it can be deduced from the Laughlin wavefunction that occupation numbers beyond $m_{ed} = 3N - 1$ are zero²¹. So in the incompressible (non-metallic) state of $\nu = 1/3$ the occupation number is zero outside the edge. We find that the momentum occupation number is

$$n(m)/n(m=0) = \begin{cases} e^{-2\pi m/\kappa_n}, & m > 0 \\ e^{2\pi m/\kappa_c} \{1 - m(1 - e^{-2\pi(\kappa_c^{-1} + \kappa_n^{-1})})\}, & m < 0. \end{cases} \quad (23)$$

Here $\kappa_{c,n}$ is defined by $\Lambda_{c,n}L$. The boundary of a compact $\nu = 1/2$ droplet coincides with $m = 0$ (m is measured from the value corresponding to the location of the edge m_{ed}). We find that the occupation number falls off linearly with m for the interior of a compact droplet, and exponentially for the outside. Fig. 6 shows momentum occupation numbers for eleven and twelve electrons at half-filling obtained from exact diagonalization as a function of $x = (k - k_{ed})R_{ed}$ (R_{ed} is the radius of the disk corresponding to m_{ed}). Monte Carlo results are shown for $N = 13$. These results show that electron occupation persists in the tail region, $x > 0$. They also show that near $x < 0$ five consecutive data points fall, to a good approximation, on a straight line, and is well approximated by a linear behavior $A + Bx$ for suitable choices of A and B , in agreement with our calculation, Eq. (23). Based on the field-theoretical calculations presented above, we expect that this ‘‘occupation tail’’ will persist in the thermodynamic limit.

VI. DISCUSSIONS

Let us first give a short summary of our results. The analyticity of the lowest Landau level wave functions and the relation between filling factor and the total angular momentum severely limits the possible forms of ground state trial wave functions. The computed occupation numbers of these wave functions are in excellent agreement with exact diagonalization results. This was verified for $N \leq 12$ at $\nu = 1/2$.

The proposed trial wave function at $\nu = 1/2$ can be tested against experiment. Low energy excited states can be constructed by following the prescription given in Yang and Lyue¹⁴. First the center of mass motion is constructed by multiplying the groundstate wave function with center of mass coordinate $Z = \sum_{i=1}^N x_i/N$. Then the Gram-Schmidt process can be utilized to construct an excited state that is orthogonal to this state and the groundstate. Higher excited states can be constructed repeating the Gram-Schmidt process. Investigating small size systems indicate that

several low energy peaks are present in the dynamic structure factor of a disk of electrons¹⁴. This feature is different from that of the $\nu = 1$ incompressible state, which has only one low energy peak. Far-infrared radiation of a quantum dot²⁵ may be used to investigate these peaks.

A naive incorporation of the linear dependence of the occupation numbers near the edge into chiral Luttinger theory suggests a value of tunneling exponent equal to 1. This value apparently agrees with experiment, but Fermi statistics will not be recovered in this naive approach. We believe that the tail in the occupation number beyond the edge must be incorporated to get the correct statistics. As far as the value of the tunneling exponent is concerned it seems that the important region is the linear region.

For other principal filling factors beside $\nu = 1/2$ the edge profiles and dynamic structure factors can be investigated along the similar line developed in this paper. It remains a theoretical challenge to test whether the proposed trial wave function is equivalent to some of the field theoretical approaches developed recently. Test of the consistency of these different approaches will deepen our understanding the exotic half-filled Landau level.

ACKNOWLEDGMENTS

This work has been supported by the KOSEF under grant 981-0207-085-2, and by Korea science and engineering foundation through the Quantum-functional Semiconductor Center at Dongguk university.

-
- ¹ B.I. Halperin, P.A.Lee, and N. Read, Phys. Rev. **47**, 7312 (1993)
² N. Read, Semicond. Sci. Technol. **9**, 1859 (1994); E. Rezayi and N. Read, Phys. Rev. Lett. **72**, 900 (1994).
³ R. Shankar and Ganpathy Murthy, Phys. Rev. Lett. **79**, 4437 (1997).
⁴ V. Pasquier and F. D. M. Haldane, Nucl. Phys. B **516**, 719 (1998).
⁵ N. Read, Phys. Rev. B **58**, 16262 (1998).
⁶ D. H. Lee, Phys. Rev. Lett. **80**, 4745 (1998).
⁷ B. I. Halperin and Ady Stern, Phys. Rev. Lett. **80**, 5457 (1998); A. Stern, B. I. Halperin, F. von Oppen, and S. H. Simon, Phys. Rev. B **59**, 12547 (1999).
⁸ M. Grayson, D.C. Tsui, L.N. Pfeiffer, K.W. West, and A.M. Chang, Phys. Rev. Lett. **80** 1062 (1998).
⁹ A.V. Shytov, L.S. Levitov, and B.I. Halperin, Phys. Rev. Lett. **80**, 141 (1998).
¹⁰ D. H. Lee and X.G. Wen; cond-mat/9809160.
¹¹ A. Lopez and E. Fradkin, Phys. Rev. B **59**, 15323 (1999).
¹² S.-R. Eric Yang and J. H. Han, Phys. Rev. B **57**, R12681 (1998).
¹³ J. H. Han and S.-R. Eric Yang, Phys. Rev. B **58**, R10163 (1998).
¹⁴ S.-R. Eric Yang and W.S. Lyue, Int. J. Mod. Phys. B, **14**, 611 (2000).
¹⁵ J. K. Jain and R. K. Kamilla, Int. J. Mod. Phys. B **11**, 2621 (1997).
¹⁶ S.-R. Eric Yang, A.H. MacDonald, M. D. Johnson, Phys. Rev. Lett. **71**, 3194 (1993).
¹⁷ G. Dev and J.K. Jain, Phys. Rev. B **45**, 1223, (1992); J.K. Jain and T. Kawamura, Europhys. Lett. **29**, 321 (1995); A. Cappelli, C. Mendez, J. Simonin, and G. R. Zemba, Phys. Rev. B **58**, 16291 (1998).
¹⁸ J. K. Jain, Phys. Rev. Lett. **63**, 199 (1989).
¹⁹ S. M. Girvin and T. Jach, Phys. Rev. B **29**, 5617 (1984).
²⁰ R. B. Laughlin, Phys. Rev. Lett. **50**, 1395 (1983).
²¹ Sami Mitra and A.H. MacDonald, Phys. Rev. B **48**, 2005 (1993);
²² X.G. Wen, Int. J. Mod. Phys. B **6** 1711 (1992).
²³ E. H. Rezayi and F.D.M. Haldane, Phys. Rev. B **50**, 17199 (1993);
²⁴ Unlike chiral edge, narrow Hall bar at $\nu = 1/3$ has power law singularities in the occupation number $n(k)$ not only near $k = \pm 3k_F$ but also near $k = \pm k_F$. See S.-R. Eric Yang, Sami Mitra, A.H. MacDonald, and M.P.A. Fisher, J. Korean Phys. Soc.**49**, S10 (1996). This result is consistent with the general description of Luttinger liquid by Haldane.
²⁵ For a review see D. Heitman and J.P. Kotthaus, Physics Today (June), 56 (1993).

TABLE I. Possible choices of $[N_0, N_1, \dots]$ at $\nu = 1/2$ and energy evaluated. $\langle \psi_a | H | \psi_a \rangle / \langle \psi_a | \psi_a \rangle$ are the energies for each wave function. E_{ED} are the energies obtained by the exact diagonalization method. Numbers in the parenthesis represent Monte Carlo error bars.

N	M_{tot}	$[N_0, N_1, \dots]$	$\langle \psi_a H \psi_a \rangle / \langle \psi_a \psi_a \rangle$	E_{ED}
3	6	[2,1]	0.891(3)	
4	12	[2,2]	1.686(3)	
5	20	[3,1,1]	2.534(4)	2.537
6	30	[3,2,1]	3.569(5)	3.567
7	42	[4,1,1,1]	4.798(6)	4.793
8	56	[4,2,1,1]	6.025(6)	6.023
		[3,3,2]	6.095(6)	
9	72	[5,1,1,1,1]	7.564(6)	7.473
		[3,3,3]	7.568(8)	
10	90	[5,2,1,1,1]	8.986(6)	8.927
		[4,3,2,1]	8.930(6)	
11	110	[6,1,1,1,1,1]	10.763(7)	10.58
		[4,3,3,1]	10.593(8)	
12	132	[6,2,1,1,1,1]	12.386(9)	12.23
		[5,3,2,1,1]	12.232(9)	
		[4,4,2,2]	12.305(9)	
13	156	[7,1,1,1,1,1,1]	14.339(14)	
		[5,3,3,1,1]	14.045(12)	
		[4,4,3,2]	14.117(13)	
14	182	[7,2,1,1,1,1,1]	16.161(16)	
		[6,3,2,1,1,1]	15.950(16)	
		[5,4,2,2,1]	15.922(16)	

TABLE II. Possible choices of $[N_0, N_1, \dots]$ at general filling factors.

N	$\nu = 2/5$	$\nu = 3/7$	$\nu = 3/5$	$\nu = 2/3$
3	-	-	-	-
4	-	[3,1]	[2,1,1]	-
5	[4,1]	-	-	[2,1,1,1]
6	-	[4,2]	[2,2,1,1]	-
7	-	[5,1,1]	[3,1,...]	-
8	[6,2]	-	-	[2,2,1,...]
9	[7,1,1]	[6,2,1][5,4]	[3,2,1,...][2,2,2,2,1]	[3,1,...]
10	-	[7,1,1,1][5,5]	[4,1,...][2,2,2,2,2]	-
11	-	-	-	-
12	[9,2,1]	[8,2,1,1]	[4,2,1,...]	[3,2,1,...]
13	[10,1,1,1]	[9,1,...]	[5,1,...]	[4,1,...]
14	-	-	-	-
15	-	[10,2,1,1,1][9,4,2][8,6,1]	[5,2,1,...][3,3,2,2,1,...][3,2,2,2,2,2,1,1]	-
16	[12,2,1,1][11,5]	[11,1,...][8,7,1]	[6,1,...][3,2,2,2,2,2,2,1]	[4,2,1,...][2,2,2,2,2,1,...]
17	[13,1,...]	-	-	[5,1,...]
18	-	[12,2,1,...][11,4,2,1][10,6,2]	[6,2,1,...][4,3,2,2,1,...][3,3,2,2,2,2,1,...]	-

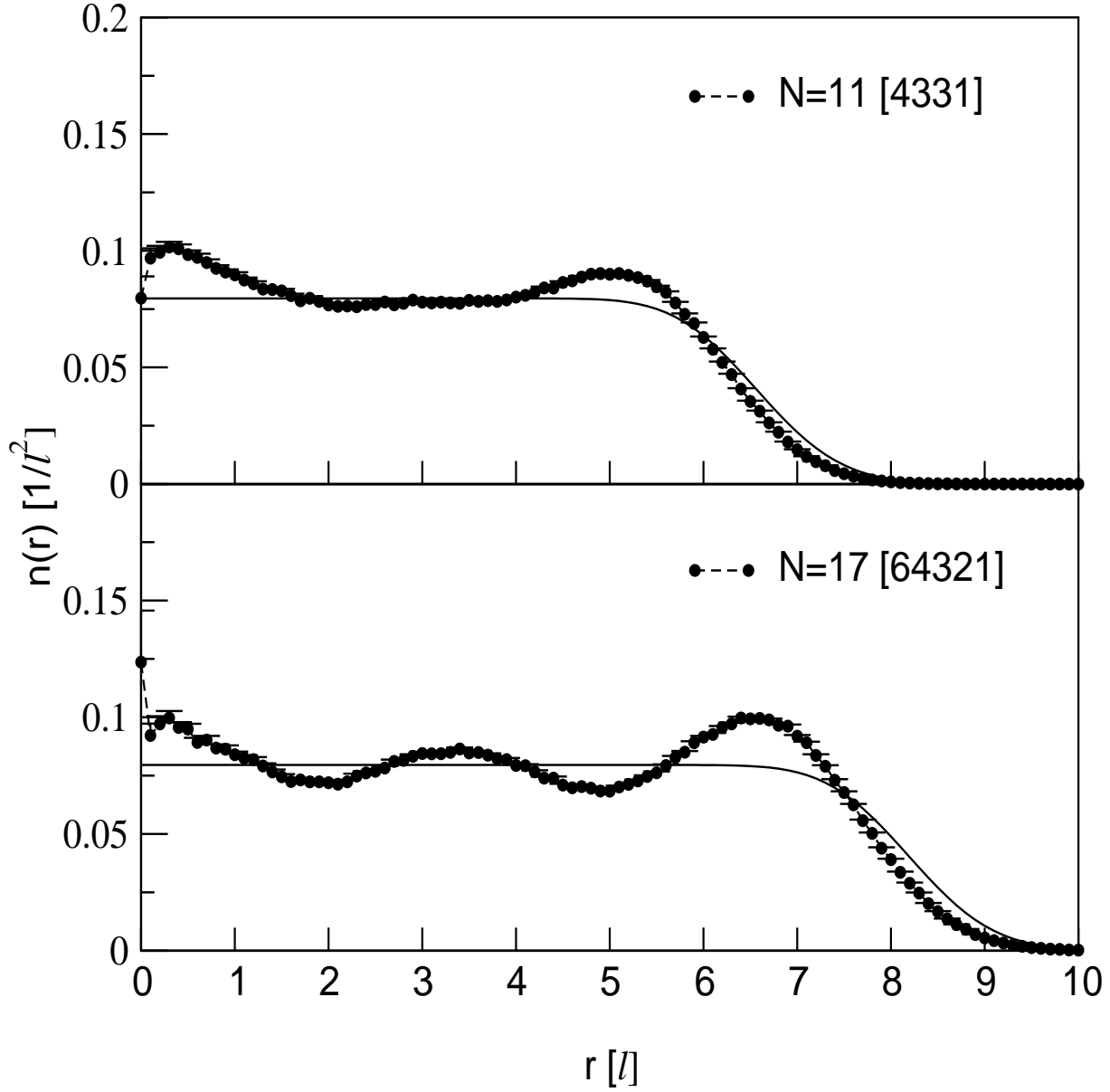


FIG. 1. The density profiles of droplets at $\nu = 1/2$ for $N = 11$ and 17. Filled circles represent the Monte Carlo calculation of trial wave functions, while the solid lines represent the expected density profile for the case that the angular momentum states are evenly occupied ($n_m = 1/2$) up to $m_{ed} = 2N - 1$. Note that, although there are some deviations between the two, the average value of the Monte Carlo results agree with the expected value. Even for the Laughlin states at $(\nu, N) = (1/3, 25)(1/5, 20)(1/7, 15)$ the density profiles have deviations from the expected value²¹.

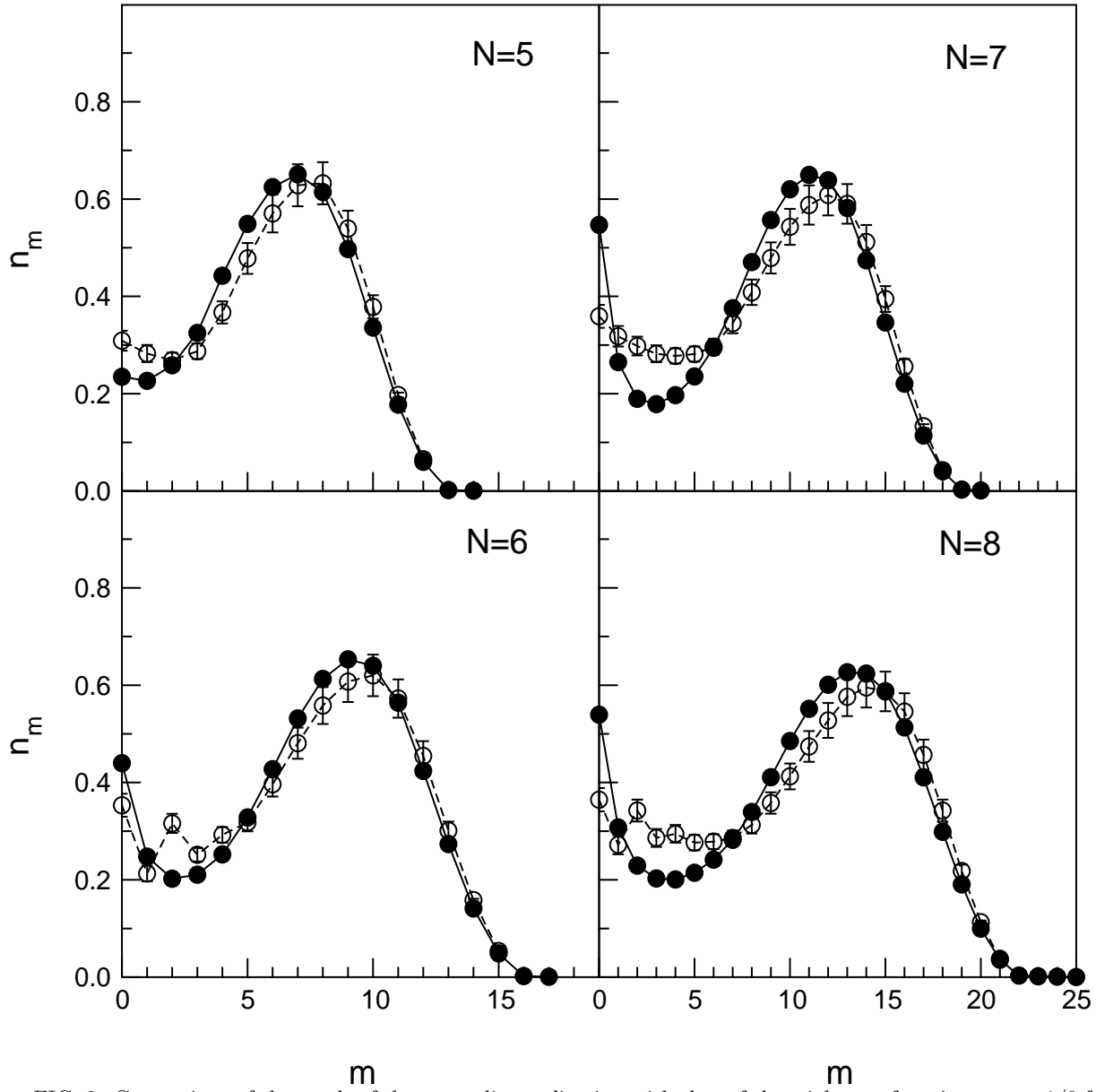


FIG. 2. Comparison of the result of the exact diagonalization with that of the trial wave function at $\nu = 1/3$ for $N = 5, 6, 7$, and 8. Filled circles represent the angular momentum occupation numbers obtained by the exact diagonalization, while the open symbols represent these quantities evaluated by a Monte Carlo method using the trial wave functions.

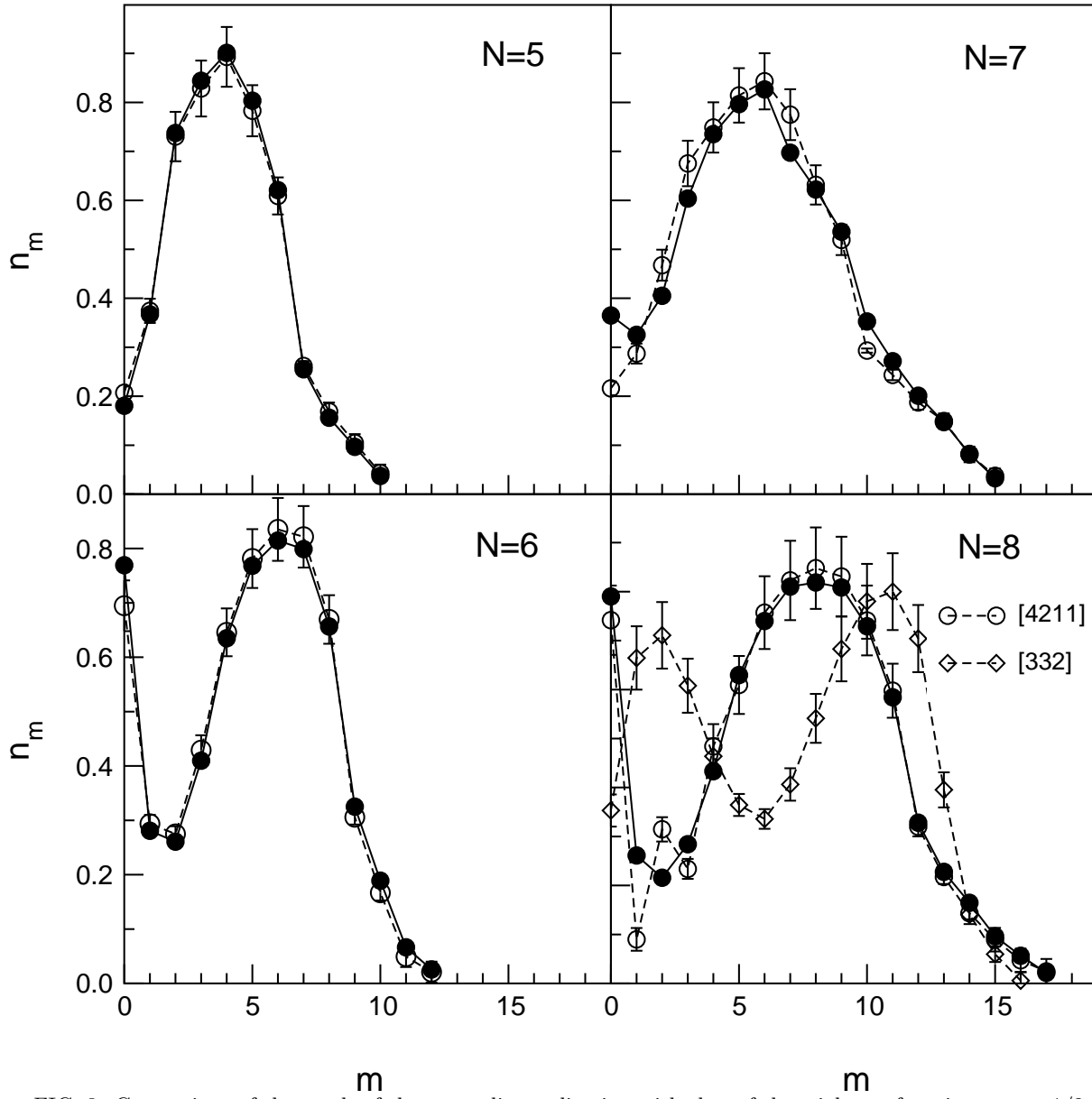


FIG. 3. Comparison of the result of the exact diagonalization with that of the trial wavefunction at $\nu = 1/2$ for $N = 5, 6, 7$, and 8 . Filled circles represent the angular momentum occupation numbers obtained by the exact diagonalization, while the open symbols represent these quantities evaluated by a Monte Carlo method using the trial wave functions. Note that for $N = 8$ there are two possible choices of the trial wave functions, among which $[4,2,1,1]$ has lower Monte Carlo energy.

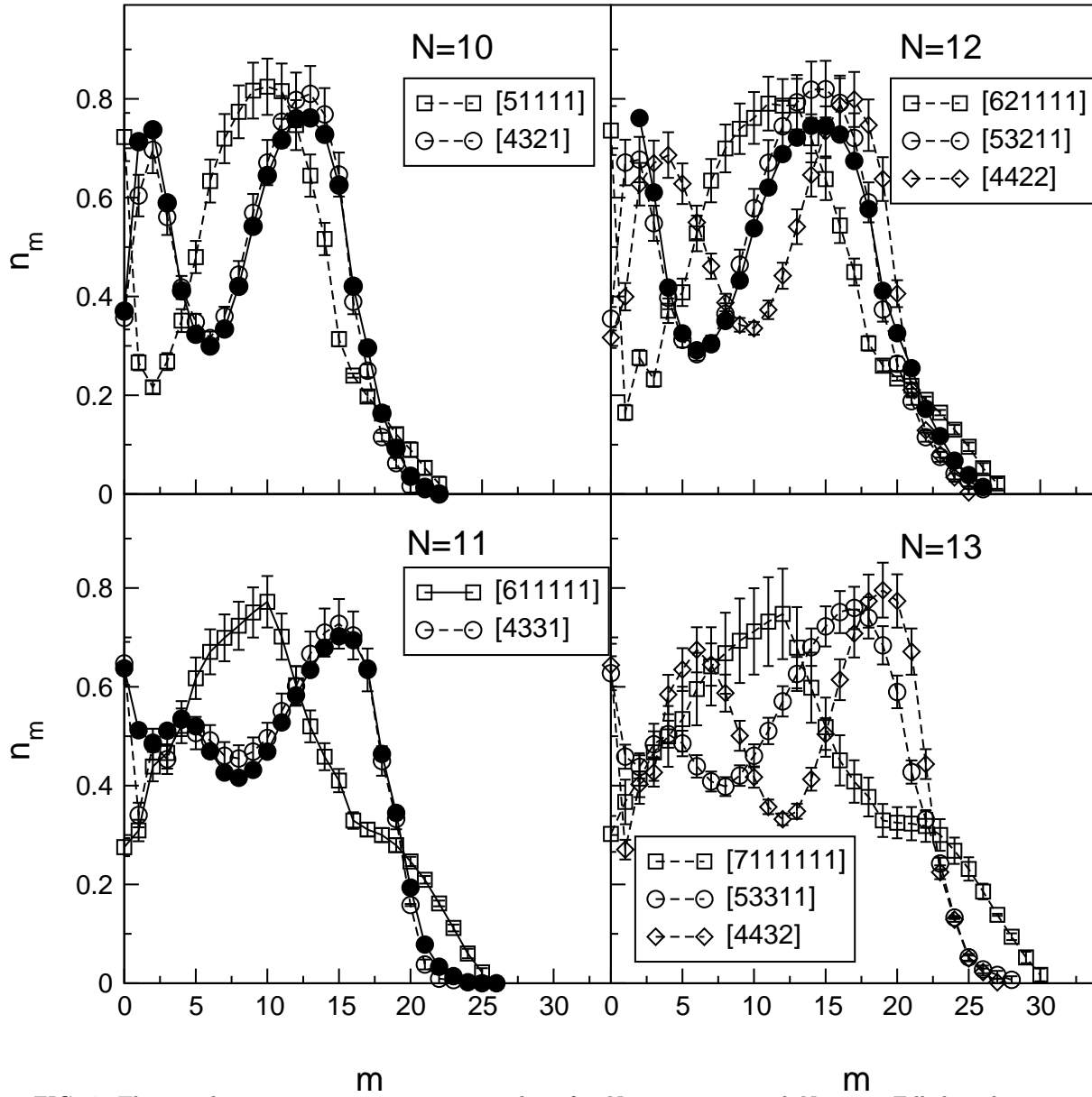


FIG. 4. The angular momentum occupation numbers for $N = 10, 11, 12$ and $N = 13$. Filled circles represent the angular momentum occupation numbers obtained by the exact diagonalization, while the open symbols represent these quantities evaluated by a Monte Carlo method using the trial wave functions. Among the possible trial wave functions, the lowest energy states give consistent results with those of the exact states.

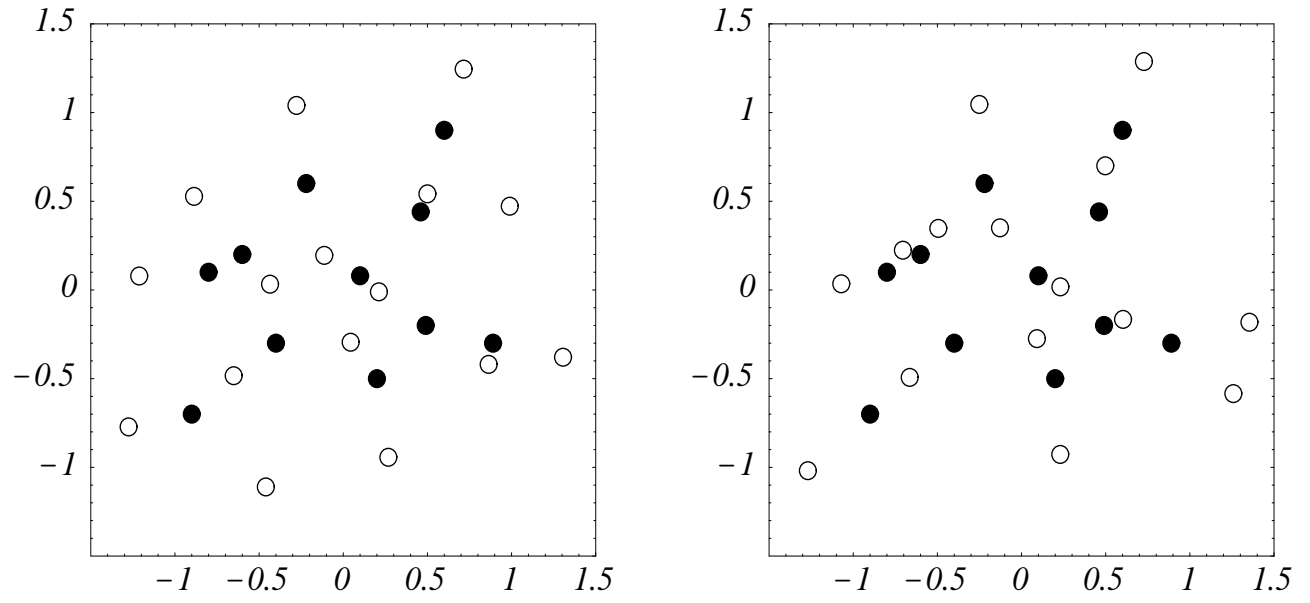


FIG. 5. A plot of zeros(\circ) for a random distribution of electrons(\bullet) for $\nu = 1/2$ and $N = 12$.

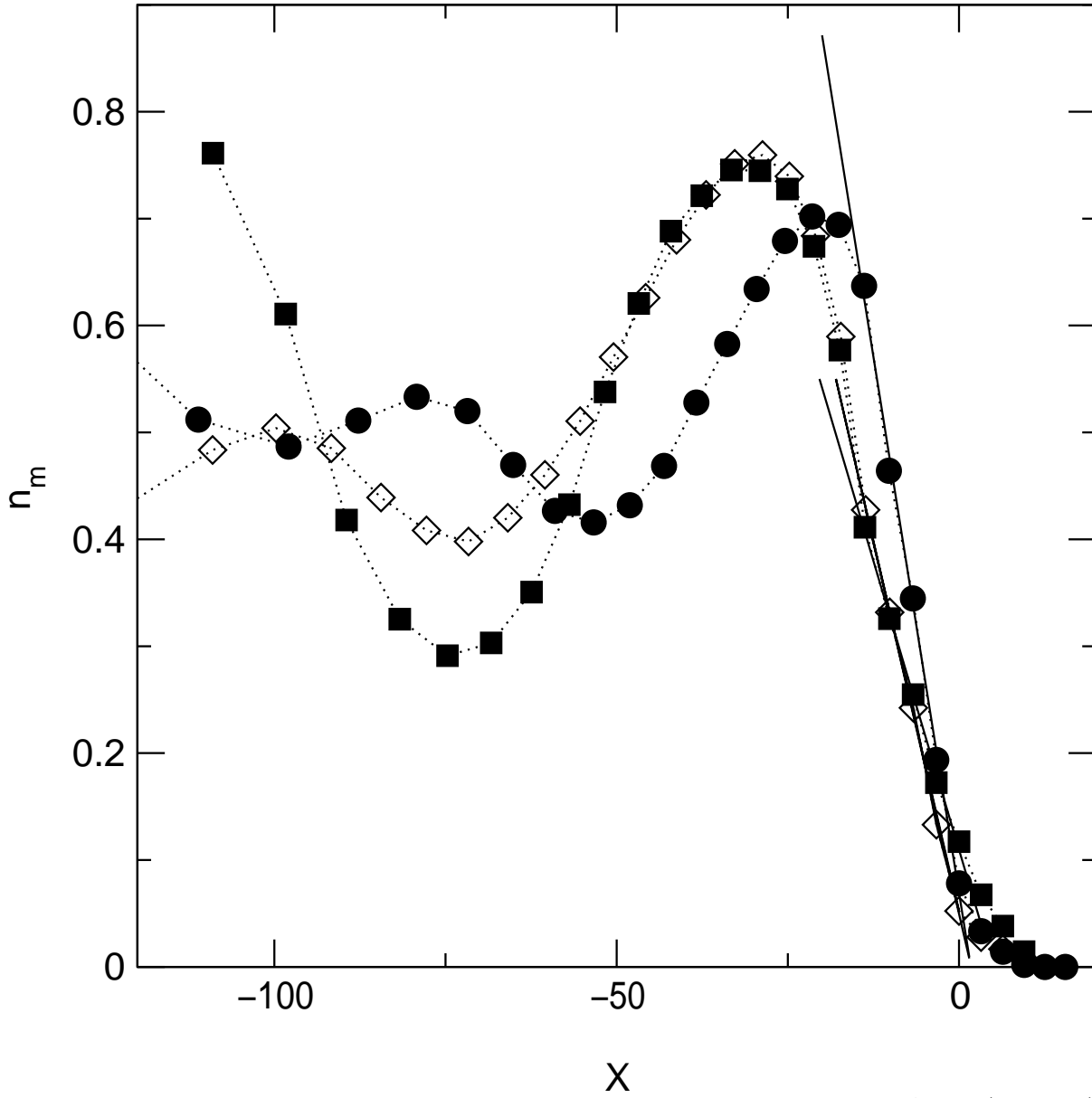


FIG. 6. The edge occupation numbers are fitted with those of a field theoretical method, $Ax + B$ (solid lines). Filled circles and squares represent the exact diagonalization results for $N = 11$ and $N = 12$, respectively, and open diamonds represent the Monte Carlo result for $N = 13$ of the trial wave function $[5,3,3,1,1]$